Direct Observation of Domain-Wall Surface Tension by Deflating or Inflating a Magnetic Bubble

Xueying Zhang,[1,2] Nicolas Vernier,[2] Weisheng Zhao,[1,*] Haiming Yu,[1] Laurent Vila,[3] Yue Zhang,[1] and Dafiné Ravelosona[2]

[1]*Fert Beijing Institute, BDBC, School of Electronic and Information Engineering, Beihang University, Beijing, China*

[2]*Centre for Nanoscience and Nanotechnology, University Paris-Saclay, 91405 Orsay, France*

[3]*University Grenoble Alpes, CEA, CNRS, Grenoble INP, INAC, SPINTEC, Grenoble 38400, France*

(Received 2 August 2017; revised manuscript received 17 November 2017; published 28 February 2018)

The surface energy of a magnetic domain wall (DW) strongly affects its static and dynamic behaviors. However, this effect is seldom directly observed, and some of the related phenomena are not well understood. Moreover, a reliable method to quantify the DW surface energy is still absent. Here, we report a series of experiments in which the DW surface energy becomes a dominant parameter. We observe that a semicircular magnetic domain bubble can spontaneously collapse under the Laplace pressure induced by DW surface energy. We further demonstrate that the surface energy can lead to a geometrically induced pinning when the DW propagates in a Hall cross or from a nanowire into a nucleation pad. Based on these observations, we develop two methods to quantify the DW surface energy, which can be very helpful in the estimation of intrinsic parameters such as Dzyaloshinskii-Moriya interactions or exchange stiffness in magnetic ultrathin films.

DOI: 10.1103/PhysRevApplied.9.024032

I. INTRODUCTION

Magnetic domain walls (DWs) in ultrathin films have attracted a lot of interest due to their potential in the development of high-density nonvolatile memory and logic applications [1–3]. A DW is the interface separating two magnetic domains, which can be moved using a magnetic field or a spin-polarized current. The fundamental behavior of a DW is similar to that of many other types of interfaces in physics, such as vortices in superconductors, soap films, or surfaces of liquids [4,5]. The properties of these interfaces have been intensively studied [6–11]. The main parameter required to explain the observed behavior is the surface energy γ. In magnetism, the effect of magnetic DW surface tension (the force associated with the surface energy) is difficult to directly observe, although it plays a very important role. For instance, the motion of DWs in the so-called creep regime results from the competition between surface energy γ, the pinning energy, and the Zeeman energy from the applied magnetic field. However, in the universal law describing DW velocity, γ is hidden in phenomenological constants [12,13]. In addition, some phenomena related to the DW surface energy are not well understood, such as DW pinning in an artificial constriction [14–16]. In particular, the surface tension of the DW plays a critical role in the topological transition of domain structures, for example, the transition from domain stripes to Skyrmionic bubbles [17]. Moreover, the stabilization and the size of these Skyrmionic bubbles are directly determined by the competition between the DW surface tension and the dipolar interaction [18].

In thin films with perpendicular magnetic anisotropy, the surface energy of a DW is given by $\gamma = 4\sqrt{AK_{\mathrm{eff}}}$, where A is the exchange stiffness and K_{eff} is the effective anisotropy energy, assuming that the DW is of Bloch type [19]. Recently, Dzyaloshinskii-Moriya interaction (DMI) has been intensively studied since it has been found to be essential in the formation of stable Skyrmions in magnetic thin films [17,20] or to obtain the high velocity of the DW motion driven by the spin Hall current [21,22]. This interaction results in an additional term in the expression of the surface energy γ that is proportional to the DMI coefficient [20,23,24]. It becomes crucial to measure γ to better understand the role of different energy terms involved in the physics of DWs and directly obtain intrinsic magnetic parameters such as the exchange stiffness A or the DMI coefficient. However, a precise and direct measurement of the surface energy is absent. In the past, the method to measure γ usually relied on gauging the size of magnetic domains at a demagnetization state [25–27]. Nevertheless, the structure of domains strongly depends on the underlying pinning potential and the manner in which the demagnetizing state is reached, which makes this approach unreliable for γ measurement.

In this work, we show that a magnetic bubble can spontaneously collapse in zero fields due to the DW surface tension and can be stabilized using an external field.

*weisheng.zhao@buaa.edu.cn

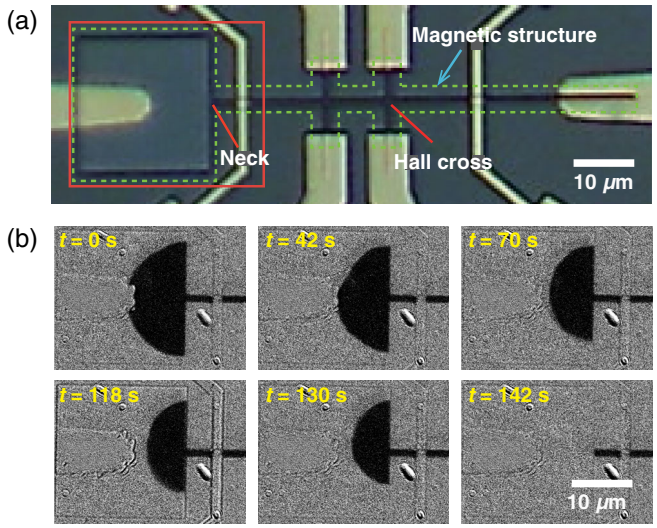

FIG. 1. (a) Optical image of one of the samples studied. The width of the wire for this sample is 1 μm. The zone surrounded by the green dashed line is the magnetic structure and that surrounded by the red line corresponds to the area viewed in (b). (b) Kerr images showing the spontaneous contraction of the semicircular domain bubble in a zero external field.

The interaction between two bubbles is also investigated. The DW depinning mechanism at the Hall cross or at the entrance of the nucleation pad is studied and explained in terms of the DW surface energy. Based on these observations, two approaches are proposed to measure the DW surface energy, one is through the dependence of the stabilizing field on the bubble size and the other is through the dependence of the depinning field on the nanowire width.

II. EXPERIMENTS AND DISCUSSIONS

A. Spontaneous contraction of the magnetic bubble

The sample studied is a Ta(5 nm)/$(Co_{40}Fe_{40})B_{20}$(1 nm)/MgO(2 nm)/Ta(5 nm) multilayer stack with perpendicular anisotropy. It is patterned into a narrow wire with Hall crosses, and the wire is connected with a nucleation pad (the square), as shown in Fig. 1(a). The size of the magnetic square is 20×20 μm^2, and the width of the wire in different structures varies from 200 nm to 1.5 μm. After obtaining a DW in the wire, we inject the DW from the narrow wire into the square by using a large field pulse. After the pulse, a semicircular bubble domain is obtained, as shown in Fig. 1(b).

Subsequently, although the magnetic field is zero, we find that the bubble can contract spontaneously until the DW returns to the entrance of the nucleation pad, i.e., the neck, as shown in Fig. 1(b). An example of this dynamic process is shown in Video 1. Furthermore, the speed of the contraction depends on the radius of the curvature of the DW circle. The smaller the radius, the faster the contraction. When the radius of the bubble is 8.8 μm, the DW contraction is observable only after 20 s. However, when the radius of the DW bubble

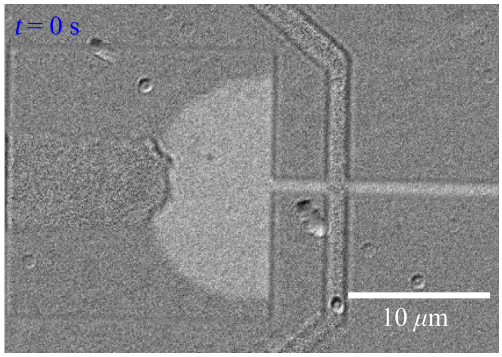

VIDEO 1. Spontaneous collapse of a semicircular domain bubble in a 20×20 μm^2 square while no external field is applied.

shrinks to 4 μm, the DW returns to the neck after several seconds. After returning to the neck, the DW does not move anymore. A Hall probe is used to check the magnetic field around the sample, and no parasitic field is found. In addition, the experiment is conducted with both directions of the magnetization of the bubble, and the result is the same, which will not be the case if there is a remnant field.

A DW can be seen as an elastic membrane with energy γ per unit area [28]. According to the physics of membranes, assuming isotropic pressure, the equilibrium for a membrane is obtained when the difference of the pressure between both sides is equal to γ/R, where R is the radius of the curvature of the membrane. Here, the interface between the domain bubble and the adjacent domain is a cylindrical surface of radius R, as shown in Fig. 2. According to the Laplace-Young equation [4,5,28], when the DW presents a curvature, a pressure is induced on the DW due to its surface energy. In the case of a cylindrical surface, this pressure is given by

$$P_\gamma = \gamma/R. \tag{1}$$

Because the bubbles created here have a quite small radius (<10 μm), this pressure is high enough to induce

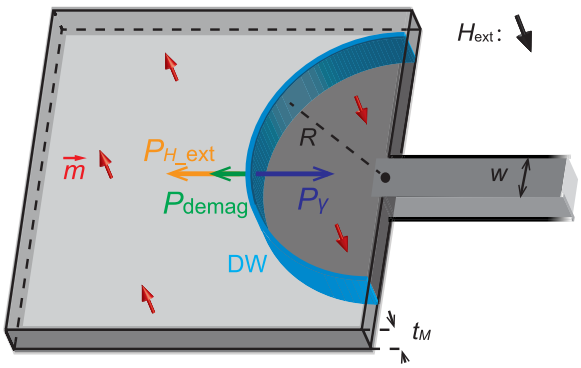

FIG. 2. 3D sketch of the profile of the semicircular magnetic bubble stabilized in the square. Arrows on the DW indicate the different pressures on this part. Since the pressures are isotropic, the direction of the local forces points perpendicularly to the surface of the DW and changes according to the position on the DW.

some movement of the bubble in the creep regime. Note that it remains a relatively low force; the movement is possible because (Co,Fe)B is very soft [29]. In agreement with $P_\gamma = \gamma/R$, the spontaneous contraction is faster as the radius of the domain is reduced.

B. Stabilization of the magnetic bubble and estimation of the DW surface energy

To quantify the Laplace pressure, the external field needed to compensate for this pressure and stabilize the domain bubble is measured, as shown in Fig. 3(a). We find that the magnitude of the external field H_{ext} required to stabilize the semicircular domain bubble depends on the size of the bubble. When H_{ext} is larger (smaller) than the stabilizing field, the domain bubble will expand (contract). In Fig. 3(c), the critical fields for expansion and for contraction are plotted as a function of the inverse of the radius of the domain bubble.

For a magnetic system, the effect of magnetic field H on a DW can be seen as a pressure of magnitude

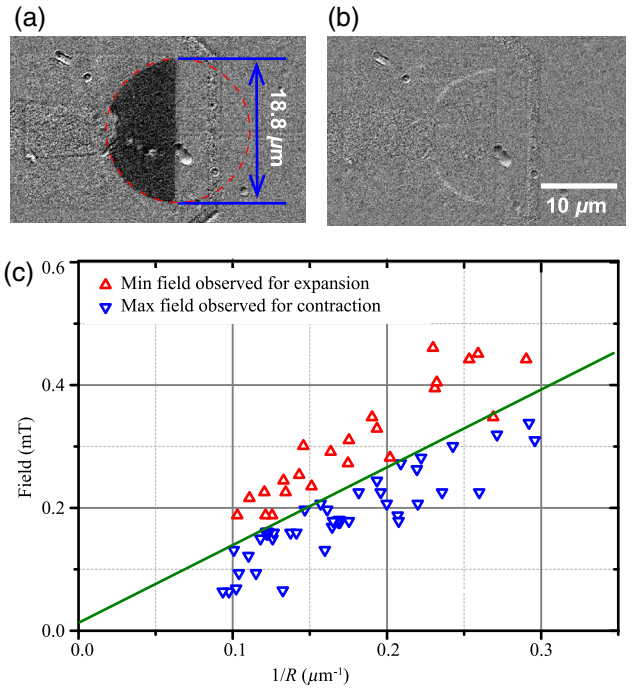

FIG. 3. (a) A semicircular bubble is stabilized by an external field $\mu_0 H_{\text{ext}} = 0.11$ mT, and no DW motion is observed during 60 s. (b) $\mu_0 H_{\text{ext}}$ decreases to 0.094 mT, and the domain bubble contracts slightly. This image is the difference between the image acquired before reducing the applied field and the image acquired 66 s after reducing the field. The white circular trace shows the DW displacement. (c) Critical fields for expansion and contraction as a function of the inverse of the radius of the semicircular domain bubble. The green line is plotted along the boundary between the expansion field and contraction field, indicating the critical field required to stabilize the semicircular bubble. Two structures associated with a 600-nm-wide wire are used to obtain more statistics.

$P_H = 2\mu_0 H M_S$. Theoretically, a circular DW is stable only when the pressure from the magnetic field exactly cancels out the Laplace pressure due to the DW surface tension. Since the Laplace pressure increases linearly as the inverse of the radius of the DW bubble, the field required to stabilize the semicircular domain bubble should be inversely proportional to its radius. In Fig. 3(c), the stabilizing field appears as the boundary between the expansion fields and contraction fields, indicated by the green line. We can see that there is very good agreement between the predicted behavior and the experimental one, the slope being $k_{\text{equ}} \approx 1.2$ mT μm.

However, there are two contributions to the magnetic field: the externally applied field and the demagnetizing field. We numerically calculate the demagnetizing field using the concept of magnetization current [30] and find that the demagnetizing field can be approximated by a linear law $\mu_0 H_{\text{demag}} \approx k_{\text{demag}}(1/R)$. For a radius R from 3 to 10 μm, the slope $k_{\text{demag}} = 1.24$ mT μm.

From the above considerations, the equilibrium of the pressures can be written as follows:

$$2\mu_0 H_{\text{ext}} M_S + 2\mu_0 H_{\text{demag}} M_S - \frac{\gamma}{R} = 0. \tag{2}$$

Using the linear laws found for $\mu_0 H_{\text{demag}} = k_{\text{demag}}/R$ and the equilibrium field $\mu_0 H_{\text{equ}} = k_{\text{equ}}/R$ and simplifying by $1/R$, the surface energy of the DW is given by

$$\gamma = 2M_S(k_{\text{equ}} + k_{\text{demag}}). \tag{3}$$

From Eq. (3), we get $\gamma \approx 5.4$ mJ/m^2. From Refs. [31,32], the exchange stiffness A in this type of material is found to be between 10 and 28 pJ/m. For our sample, the effective anisotropy is measured as $K_{\text{eff}} = 2.2 \times 10^5$ J/m^3 [33]. The formula $\gamma = 4\sqrt{AK_{\text{eff}}}$ gives γ between 6 and 10 mJ/m^2. It can be seen that our value is in good agreement with the theoretically calculated one. The uncertainty of the measured γ is expected to be less than 10% [30]. Indeed, with the progress of technologies of Kerr microscopy [34,35], the precision can be further improved. Note that the formula used here to calculate γ applies only to films without DMI. In fact, the DMI constant measured in our system is less than 0.01 mJ/m^2, implying that its effect on the DW surface energy is negligible [36].

C. Interaction of two domain bubbles

As suggested before, the behavior of magnetic bubbles induced by the surface energy is similar to that of soap bubbles. There is a well-known experiment in which two soap bubbles are connected to each other via a tube. Instead of obtaining two bubbles of equal size, the smaller bubble contracts while the bigger one expands due to the unbalanced Laplace pressure [4,5,37]. Here, we observe the same phenomenon. We simultaneously create two semicircular bubbles with different sizes in a magnetic square, as shown

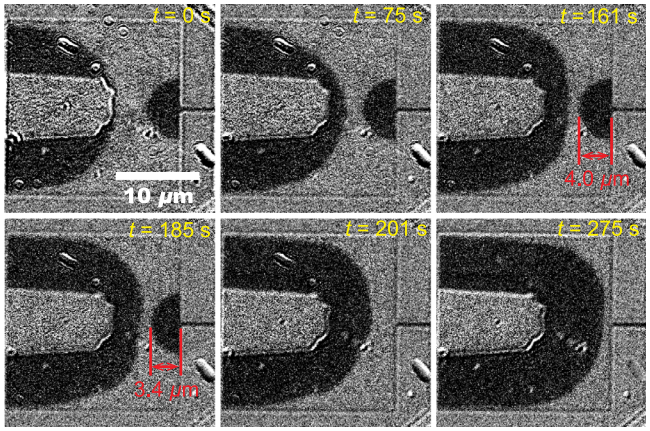

FIG. 4. Interaction of two semicircular domain bubbles. Under an applied field of 0.41 mT, the bigger bubble expands and squeezes the smaller one.

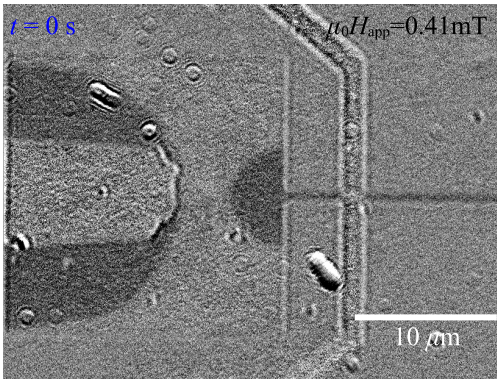

VIDEO 2. Dynamic process of the interaction of two semicircular domain bubbles with different size. This video corresponds to the images sequence shown in Fig. 4.

in Fig. 4. An external field $\mu_0 H_{\text{ext}} = 0.41$ mT is applied to avoid the collapse of both bubbles. In the beginning, the smaller magnetic bubble is stable while the larger one expands slowly. When the two bubbles get close, the bigger bubbles continue to expand while the smaller one contracts back to the neck. Video 2 shows this dynamic process.

The competition of three pressures governs this process: the Zeeman pressure tends to enlarge the size of both bubbles; the repulsive pressure between the two bubbles due to dipolar interaction [38] hinders the merger of the two bubbles; the Laplace pressure tends to reduce the sizes of the bubbles. The strength of the former two pressures is equal for the two bubbles while the Laplace pressure is higher for the smaller bubble, as predicted by Eq. (1). Finally, the smaller bubble is squeezed by the larger one.

D. DW depinning at the neck or Hall crosses

Eventually, we conduct an experiment revealing that the DW pinning and depinning processes in some artificial structures are governed by the DW surface energy. We find

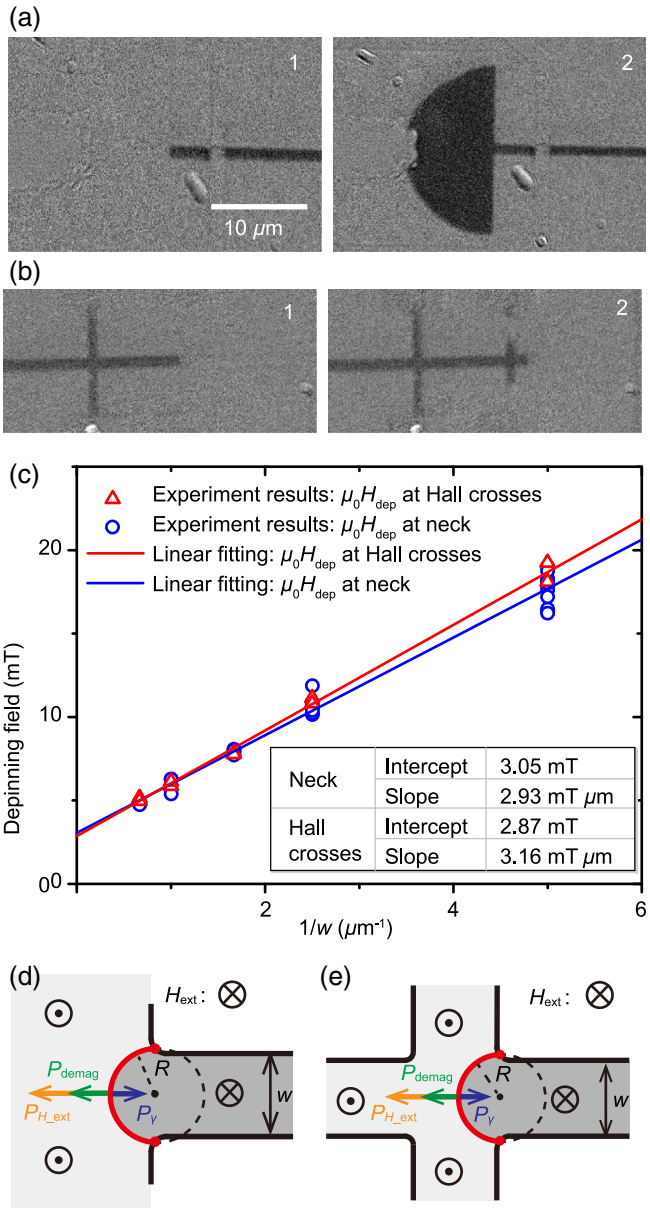

FIG. 5. (a),(b) DW depinning at the neck (Hall cross). Image 1 shows the pinned DW after a field pulse of 5.8 mT (5.9 mT) and 5 μs; image 2 shows the profile of the DW depinned after the magnitude of the field pulse increases to 5.9 mT (6.0 mT). (c) DW depinning field as a function of the inverse of the wire width. (d),(e) Sketches of pressures acting on the DW pinned at the corners of a neck or a Hall cross, respectively. It can be seen that the minimum radius (corresponding to the highest Laplace pressure possible) of these circular arcs is $w/2$.

that when injecting a DW from the narrow wire into the square, the DW is pinned at the neck and will not be depinned until the applied field reaches a threshold value [Fig. 5(a)]. This threshold field is defined as the DW depinning field H_{dep} here. Note that the duration of the field pulse is always 5 μs in these measurements. For Hall crosses, the behavior is the same [Fig. 5(b)]: pinning if H_{ext} is below a critical field and movement above it.

Interestingly, the depinning field depends on the width w of the wire, as plotted in Fig. 5(c). It can be seen that there is a linear dependence of H_{dep} as a function of the inverse of the width. Furthermore, the dependence is almost the same for the Hall cross as it is for the neck. Note that when $1/R$ tends to zero, the depinning field tends to $\mu_0 H_0 = 3$ mT. This value is close to the intrinsic pinning field of the film structure, below which the DW velocity obeys the creep law and no sufficient movement can occur for depinning [33].

Now, our experiments show that the pinning is due to the DW surface energy. We can do the same analysis as the stabilization of a domain bubble. In this case, the minimum radius of the bubble is $w/2$, where w is the wire width [see Figs. 5(d) and 5(e)]. Therefore, the maximum Laplace pressure induced by the DW surface tension is $2\gamma/w$. Movement and depinning from the neck can occur only if the overall pressure due to the magnetic field (including H_{ext} and H_{demag}) and Laplace pressure is larger than the pressure induced by H_0 alone,

$$2\mu_0 H_{ext} M_S + 2\mu_0 H_{demag} M_S - \frac{2\gamma}{w} \geq 2\mu_0 H_0 M_S. \quad (4)$$

The depinning field is predicted to be

$$\mu_0 H_{dep} = \frac{\gamma}{M_S w} - \mu_0 H_{demag} + \mu_0 H_0. \quad (5)$$

As before, H_{demag} is numerically calculated, and we again find an approximate linear law: $\mu_0 H_{demag} \approx k_{demag}/w$, where $k_{demag} = 0.84$ mT μm in the case of pinning at the neck and $k_{demag} = 0.58$ mT μm at the Hall crosses,

$$\mu_0 H_{dep} = \left(\frac{\gamma}{M_S} - k_{demag}\right)\frac{1}{w} + \mu_0 H_0. \quad (6)$$

This prediction fits perfectly with our experimental results. With the slope $k = 2.9$ mT μm for necks (3.2 mT μm for Hall crosses) found experimentally, the surface tension γ can be calculated,

$$\gamma = M_S(k + k_{demag}). \quad (7)$$

It gives $\gamma = 4.1$ mJ/m^2, which is consistent with our previous results. The slight discrepancy can arise from the edges of the Hall crosses, which are probably slightly rounded, inducing a small enlargement of the width of the wire at the entrance of the cross or nucleation pad [30].

III. CONCLUSION

To conclude, we directly observe the spontaneous contraction of semicircular domain bubbles induced by the DW surface tension. The field required to stabilize the domain bubble is used to quantify the DW surface energy, which gives $\gamma = 5.4$ mJ/m^2 for our sample. The interaction of two bubbles under the competition of the DW surface tension and the dipolar repulsion is demonstrated. In addition, the pinning of the DW at the Hall crosses or at the neck between a narrow wire and a large pad is explained in terms of the DW surface tension. The linear dependence of the DW depinning field on the wire width is used to measure the DW surface energy, giving $\gamma = 4.1$ mJ/m^2, consistent with the previous measurement result. Our experiments reveal the important effect of the DW surface energy on the DW behavior, and our method for the surface energy measurement can be very helpful in studying thin films presenting DMI, since these interactions change the surface energy drastically [30].

This work is supported in part by the National Natural Science Foundation of China (Grants No. 61501013, No. 61571023, and No. 61627813) and the China Scholarship Council. The authors also gratefully acknowledge the International Collaboration Projects No. 2015DFE12880 and No. B16001. We also acknowledge the support from the Renatec network for the sample fabrication.

[1] S. Parkin and S.-H. Yang, Memory on the racetrack, Nat. Nanotechnol. **10**, 195 (2015).
[2] J. H. Franken, H. J. M. Swagten, and B. Koopmans, Shift registers based on magnetic domain wall ratchets with perpendicular anisotropy, Nat. Nanotechnol. **7**, 499 (2012).
[3] S. S. P. Parkin, M. Hayashi, and L. Thomas, Magnetic domain-wall racetrack memory, Science **320**, 190 (2008).
[4] C. Isenberg, *The Science of Soap Films and Soap Bubbles*, 2nd ed. (Dover Publications, Inc., New York, 1992).
[5] P.-G. de Gennes, F. Brochard-Wyart, and D. Quéré, *Capillarity and Wetting Phenomena* (Springer-Verlag, New York, 2004).
[6] F. Fan, E. J. R. Parteli, and T. Pöschel, Origin of Granular Capillarity Revealed by Particle-Based Simulations, Phys. Rev. Lett. **118**, 218001 (2017).
[7] N. Taccoen, F. Lequeux, D. Z. Gunes, and C. N. Baroud, Probing the Mechanical Strength of an Armored Bubble and Its Implication to Particle-Stabilized Foams, Phys. Rev. X **6**, 011010 (2016).
[8] R. W. Style, R. Boltyanskiy, Y. Che, J. S. Wettlaufer, L. A. Wilen, and E. R. Dufresne, Universal Deformation of Soft Substrates Near a Contact Line and the Direct Measurement of Solid Surface Stresses, Phys. Rev. Lett. **110**, 066103 (2013).
[9] T. Koyama, D. Chiba, K. Ueda, K. Kondou, H. Tanigawa, S. Fukami, T. Suzuki, N. Ohshima, N. Ishiwata, Y. Nakatani, K. Kobayashi, and T. Ono, Observation of the intrinsic pinning of a magnetic domain wall in a ferromagnetic nanowire, Nat. Mater. **10**, 194 (2011).
[10] F. Blanchette and T. P. Bigioni, Partial coalescence of drops at liquid interfaces, Nat. Phys. **2**, 254 (2006).
[11] I. Akhatov, N. Gumerov, C. D. Ohl, U. Parlitz, and W. Lauterborn, The Role of Surface Tension in Stable Single-Bubble Sonoluminescence, Phys. Rev. Lett. **78**, 227 (1997).

[12] S. Lemerle, J. Ferré, C. Chappert, V. Mathet, T. Giamarchi, and P. Le Doussal, Domain Wall Creep in an Ising Ultrathin Magnetic Film, Phys. Rev. Lett. **80**, 849 (1998).
[13] S. DuttaGupta, S. Fukami, C. Zhang, H. Sato, M. Yamanouchi, F. Matsukura, and H. Ohno, Adiabatic spin-transfer-torque-induced domain wall creep in a magnetic metal, Nat. Phys. **12**, 333 (2016).
[14] S. Sangiao and M. Viret, Electrical detection of internal dynamical properties of domain walls, Phys. Rev. B **89**, 104412 (2014).
[15] K. J. O'Shea, J. Tracey, S. Bramsiepe, and R. L. Stamps, Probing nanowire edge roughness using an extended magnetic domain wall, Appl. Phys. Lett. **102**, 062409 (2013).
[16] C. Burrowes, A. P. Mihai, D. Ravelosona, J.-V. Kim, C. Chappert, L. Vila, A. Marty, Y. Samson, F. Garcia-Sanchez, L. D. Buda-Prejbeanu, I. Tudosa, E. E. Fullerton, and J.-P. Attané, Non-adiabatic spin-torques in narrow magnetic domain walls, Nat. Phys. **6**, 17 (2010).
[17] W. Jiang, P. Upadhyaya, W. Zhang, G. Yu, M. B. Jungfleisch, F. Y. Fradin, J. E. Pearson, Y. Tserkovnyak, K. L. Wang, O. Heinonen, S. G. E. te Velthuis, and A. Hoffmann, Blowing magnetic Skyrmion bubbles, Science **349**, 283 (2015).
[18] A. Fert, N. Reyren, and V. Cros, Magnetic Skyrmions: Advances in physics and potential applications, Nat. Rev. Mater. **2**, 17031 (2017).
[19] A. Hubert and R. Schäfer, *Magnetic Domains, The Analysis of Magnetic Microstructures* (Springer, New York, 2009).
[20] S. Rohart and A. Thiaville, Skyrmion confinement in ultrathin film nanostructures in the presence of Dzyaloshinskii-Moriya interaction, Phys. Rev. B **88**, 184422 (2013).
[21] E. Martinez, S. Emori, N. Perez, L. Torres, and G. S. D. Beach, Current-driven dynamics of Dzyaloshinskii domain walls in the presence of in-plane fields: Full micromagnetic and one-dimensional analysis, J. Appl. Phys. **115**, 213909 (2014).
[22] E. Jué, A. Thiaville, S. Pizzini, J. Miltat, J. Sampaio, L. D. Buda-Prejbeanu, S. Rohart, J. Vogel, M. Bonfim, O. Boulle, S. Auffret, I. M. Miron, and G. Gaudin, Domain wall dynamics in ultrathin Pt/Co/AlO_x microstrips under large combined magnetic fields, Phys. Rev. B **93**, 014403 (2016).
[23] D. S. Han, N. H. Kim, J. S. Kim, Y. Yin, J. W. Koo, J. Cho, S. Lee, M. Kläui, H. J. M. Swagten, B. Koopmans, and C. Y. You, Asymmetric hysteresis for probing Dzyaloshinskii-Moriya interaction, Nano Lett. **16**, 4438 (2016).
[24] F. Hellman, A. Hoffmann, Y. Tserkovnyak, G. S. D. Beach, E. E. Fullerton, C. Leighton, A. H. Macdonald, D. C. Ralph, D. A. Arena, and H. A. Dürr, Interface-induced phenomena in magnetism, Rev. Mod. Phys. **89**, 025006 (2017).
[25] M. Yamanouchi, A. Jander, P. Dhagat, S. Ikeda, F. Matsukura, and H. Ohno, Domain structure in CoFeB thin films with perpendicular magnetic anisotropy, IEEE Magn. Lett. **2**, 3000304 (2011).
[26] S. Haghgoo, M. Cubukcu, H. J. Von Bardeleben, L. Thevenard, A. Lemaître, and C. Gourdon, Exchange constant and domain wall width in (Ga,Mn)(As,P) films with self-organization of magnetic domains, Phys. Rev. B **82**, 041301 (2010).
[27] B. Kaplan and G. A. Gehring, The domain structure in ultrathin magnetic films, J. Magn. Magn. Mater. **128**, 111 (1993).
[28] P. Gaunt, The frequency constant for thermal activation of a ferromagnetic domain wall, J. Appl. Phys. **48**, 3470 (1977).
[29] P. J. Metaxas, J. P. Jamet, A. Mougin, M. Cormier, J. Ferré, V. Baltz, B. Rodmacq, B. Dieny, and R. L. Stamps, Creep and Flow Regimes of Magnetic Domain-Wall Motion in Ultrathin Pt/Co/Pt Films with Perpendicular Anisotropy, Phys. Rev. Lett. **99**, 217208 (2007).
[30] See Supplemental Material at http://link.aps.org/supplemental/10.1103/PhysRevApplied.9.024032 for more detailed information about the experiments, the method to calculate the stray field, the analysis of uncertainties of the results, and the potential application of these experiments to the extraction of intrinsic parameters of materials, such as the strength of DMI.
[31] C.-Y. You, Dependence of the switching current density on the junction sizes in spin transfer torque, Appl. Phys. Express **5**, 103001 (2012).
[32] C. Bilzer, T. Devolder, J.-V. Kim, G. Counil, C. Chappert, S. Cardoso, and P. P. Freitas, Study of the dynamic magnetic properties of soft CoFeB films, J. Appl. Phys. **100**, 053903 (2006).
[33] C. Burrowes, N. Vernier, J. P. Adam, L. Herrera Diez, K. Garcia, I. Barisic, G. Agnus, S. Eimer, J. Von Kim, T. Devolder, A. Lamperti, R. Mantovan, B. Ockert, E. E. Fullerton, and D. Ravelosona, Low depinning fields in Ta-CoFeB-MgO ultrathin films with perpendicular magnetic anisotropy, Appl. Phys. Lett. **103**, 182401 (2013).
[34] E. Nikulina, O. Idigoras, P. Vavassori, A. Chuvilin, and A. Berger, Magneto-optical magnetometry of individual 30 nm cobalt nanowires grown by electron beam induced deposition, Appl. Phys. Lett. **100**, 142401 (2012).
[35] P. Vavassori, M. Pancaldi, M. J. Perez-Roldan, A. Chuvilin, and A. Berger, Remote magnetomechanical nanoactuation, Small **12**, 1013 (2016).
[36] J.-P. Tetienne, T. Hingant, L. J. Martínez, S. Rohart, A. Thiaville, L. H. Diez, K. Garcia, J.-P. Adam, J.-V. Kim, J.-F. Roch, I. M. Miron, G. Gaudin, L. Vila, B. Ocker, D. Ravelosona, and V. Jacques, The nature of domain walls in ultrathin ferromagnets revealed by scanning nanomagnetometry, Nat. Commun. **6**, 6733 (2015).
[37] Experiments about the interplay of two soap bubbles under unbalanced Laplace pressure, https://www.youtube.com/watch?v=X4bHRPr9P0I.
[38] N. Vernier, J. P. Adam, S. Eimer, G. Agnus, T. Devolder, T. Hauet, B. Ocker, F. Garcia, and D. Ravelosona, Measurement of magnetization using domain compressibility in CoFeB films with perpendicular anisotropy, Appl. Phys. Lett. **104**, 122404 (2014).